

# Contact Splitting and the Effect of Dimple Depth on Static Friction of Textured Surfaces

Christian Greiner,<sup>\*,†</sup> Michael Schäfer,<sup>†</sup> Uwe Popp,<sup>†</sup> and Peter Gumbsch<sup>†,‡</sup>

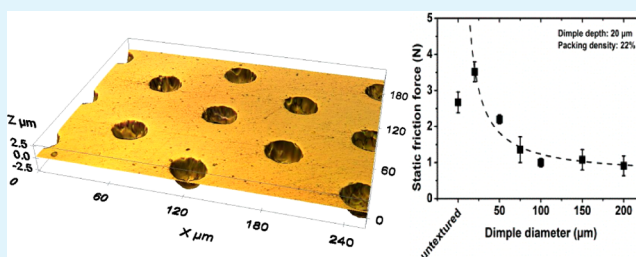
<sup>†</sup>Institute for Applied Materials IAM, Karlsruhe Institute of Technology (KIT), Kaiserstrasse 12, 76131 Karlsruhe, Germany

<sup>‡</sup>Fraunhofer IWM, Woehlerstrasse 11, 79108 Freiburg, Germany

## Supporting Information

**ABSTRACT:** The morphological texturing of surfaces has demonstrated its high potential to maximize adhesion as well as to reduce friction and wear. A key to understanding such phenomena is a principle known as contact splitting. Here, we extend this concept to the static friction behavior of dimpled surfaces. Our results indicate that contact splitting does exist for such structures and that with certain dimple sizes and depths static friction values significantly exceeding those of untextured surfaces can be obtained. These results can be applied to all surfaces where friction forces are to be tuned, from nanoelectromechanical systems up to combustion engines.

**KEYWORDS:** static friction, contact splitting, contact mechanics, brass, laser surface texturing



The morphological texturing of surfaces is of paramount importance in many fields of micro- and nanotechnology. Prominent examples are gecko-inspired dry adhesives and the texturing of sliding surfaces in order to reduce friction and wear. For dry adhesives, surfaces are patterned with pillars or similar structures and adhesive forces exceeding those of the gecko have been reported, as reviewed by Boesel et al.<sup>1</sup> Their ability to scale walls and ceilings is mainly based on van der Waals forces.<sup>2,3</sup> Some insects also rely on the secretion of oily fluids<sup>4</sup> and even for geckos, there is an influence of ambient humidity on the adhesion force of single attachment hairs (called setae) which was explained by capillary contributions.<sup>5</sup> The physical principle behind fibrillar adhesives is called contact splitting.<sup>6,7</sup> It exploits that the adhesive force of many small contacts is larger than that of one large contact. This theory was tested extensively for polymer- and carbon nanotube-based structures.<sup>8</sup> For adhesives, one usually aims at maximizing adhesion and (static) friction forces. The surfaces are dominantly textured with protruding and independent features like the above-mentioned pillars but contact splitting was also tested experimentally for elastomeric samples featuring dimples of different sizes.<sup>9,10</sup> These samples have a striking resemblance with the structures investigated in the field of laser surface texturing. The morphological laser texturing of surfaces is often used to minimize (dynamic) friction forces (and wear rates),<sup>11</sup> mainly for lubricated contacts of metals and ceramics<sup>12–14</sup> and for applications such as piston cylinder systems,<sup>12,15</sup> mechanical seals<sup>16</sup> and clutches.<sup>17</sup> It is assumed that dimpled surfaces extend the range of hydrodynamic lubrication.<sup>11,18</sup> However, at the dead centers of a reciprocating motion, there is no hydrodynamic lubrication and a solid–solid contact of the two sliding partners occurs. This leads to the

question whether laser texturing influences the transition from static to dynamic friction, whether there is a contact splitting phenomenon for these surfaces and how it influences friction behavior. We address this problem experimentally, focusing on the effect of different dimple diameters and depths on static friction between sapphire and brass. Our study reveals that there indeed is a contact splitting phenomenon for dimpled surfaces at the transition from static to dynamic friction, even though in contrast to fibrillar adhesives the contact area in our case remains connected. Under certain conditions, dimpled surfaces exhibit higher static friction forces than polished controls. This result implies that some textures might be counterproductive for reducing friction, especially at the dead centers of a reciprocating tribological contact where already most wear is observed. These findings have significant relevance for tribological and adhesive contacts ranging from large-scale applications like combustion engines, down to moving parts in micro- and nanoelectromechanical systems.

The influence of a morphological surface texture on static friction was addressed by laser surface texturing brass (Cu with 36 wt % Zn) samples. They were purchased from KGM (Fulda, Germany) in the form of 8 mm diameter spheres. To have enough area available for texturing and to achieve a flat-on-flat contact, we polished these spheres down to a circular area of 7.2 mm in diameter. The last polishing step was conducted with a colloidal SiO<sub>2</sub> suspension (OP-U from Struers, Willich, Germany), resulting in a scratch free surface having a surface roughness  $R_a < 0.01 \mu\text{m}$ .

**Received:** February 11, 2014

**Accepted:** May 19, 2014

**Published:** May 19, 2014



Laser surface texturing was carried out on the flattened end of the spheres with a Q-switched Ytterbium fiber laser (Piranha II, Acsys Instruments, Kornwestheim, Germany) at a wavelength of 1.064  $\mu\text{m}$  and a power of 20 W with the specifics of the texturing process depending of the specific texture (see the Supporting Information for details). For one set of samples, the dimple diameter was set constant at 50  $\mu\text{m}$  and the depth was varied between 10 and 65  $\mu\text{m}$ . The packing density was 22% for all samples. To investigate the dimple diameter's effect, we prepared samples with diameters of 20, 50, 75, 100, 150, and 200  $\mu\text{m}$ . Here, the dimple depth was kept constant at 20  $\mu\text{m}$ . The debris that formed during the laser ablation process was removed through polishing with a 1  $\mu\text{m}$  diamond and a 0.05  $\mu\text{m}$  colloidal silica suspension.

The static friction tests of the flattened brass spheres were performed against polished sapphire discs provided by GWI (Lauf, Germany) as counter surfaces. These discs were chosen as they exhibit extremely small surface roughness (root-mean-square roughness below 10 nm as measured by atomic force microscopy). In friction experiments,<sup>17</sup> sapphire has proven to be mechanically very stable because of its high hardness and single-crystalline character, making it an ideal counter body for fundamental tribological studies like ours.

For each sample, the exact dimple dimensions (diameter, depth and packing density) were assessed by means of white light interferometry (Sensofar Pl $\mu$  neoX, Barcelona, Spain and a FRT MicroProf, Bergisch Gladbach, Germany) as well as by digital optical microscopy (VHX-600 from Keyence, Osaka, Japan) and scanning electron microscopy (FEI Quanta 650 and Helios 650, Hillsboro, OR, USA). Optical microscopy and profilometry were also used to investigate the samples after the experiments. No signs of wear were detected.

Static friction force values were measured with a custom-built tribometer.<sup>19</sup> The experiments were conducted with a traction speed of 1  $\mu\text{m}/\text{s}$  and for a constant normal load of 10 N applied through a dead weight. Ambient temperature and relative humidity (RH) were kept constant during all experiments at 19  $^{\circ}\text{C}$  and 50% RH. The sapphire discs were fixed to the moving ground plate of the tribometer while the flattened sphere was attached to the lever arm of the tribometer in a special sample holder. The spheres were glued into this holder by making use of a fast curing two part epoxy (Uhu plus sofort fest, Buehl, Germany). Great care was taken in this process in order to ensure a true flat-on-flat contact between the sapphire discs and the brass samples. The discs were divided into 12 sectors and in each sector 10 individual measurements were carried out, yielding a total of 120 measurements for each sample. All measured data were analyzed using custom MatLab (MathWorks, Natick, MA, USA) code and the average values as well as the standard deviations were calculated.

Scanning electron microscopy and optical profilometry images of representative textures are presented in Figure 1. It demonstrates that the laser surface texturing and debris removal process was performed successfully. The samples were extremely uniform and featured dimples of precise geometrical parameters. That the laser surface texturing did not result in any large-scale waviness is shown in Figure S2 of the Supporting Information section.

During a static friction test with the flattened brass spheres in contact with a sapphire disc, the friction force increased until it reached a local maximum followed by a sudden drop and the onset of the dynamic friction regime. A typical result of such an experiment is presented in Figure S1 of the Supporting

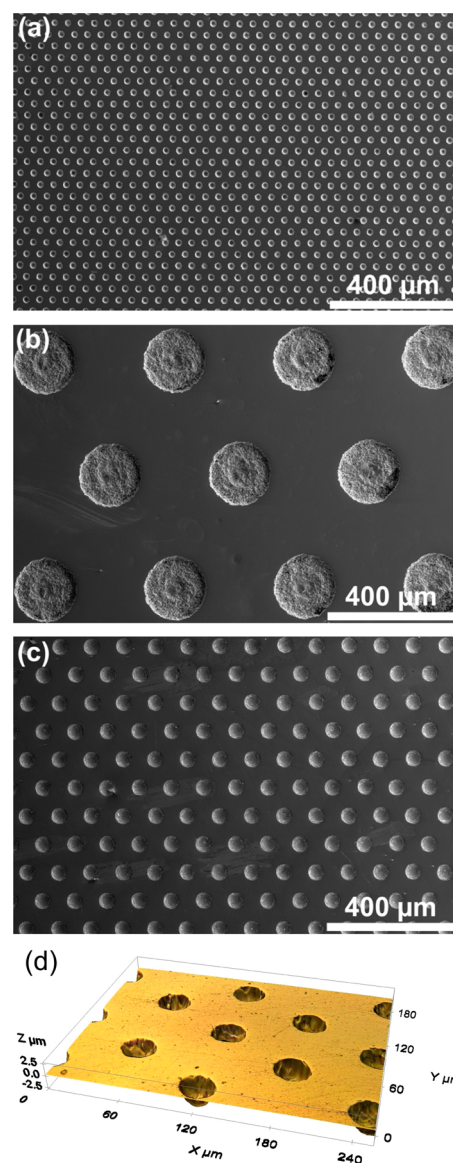


**Figure 1.** SEM and optical profilometry images of the laser textured surfaces. Textured brass (36 wt % Zn) samples with circular dimples of (a) 20  $\mu\text{m}$ , (b) 200  $\mu\text{m}$ , and (c, d) 50  $\mu\text{m}$  in diameter. In a and b, the dimples have a depth of 20  $\mu\text{m}$ , in c and d, 10  $\mu\text{m}$ . The dimple packing density is 22% for all samples tested.

Information section. As the lateral displacement of the sample was also monitored by means of capacitive sensors, we were able to detect the sudden lateral displacement coinciding with the local maximum in friction force; together strong indicators for the transition from static to dynamic friction.

To investigate the occurrence of a contact splitting phenomenon in dimpled surfaces, we measured the static friction for samples having dimple diameters between 20 and 200  $\mu\text{m}$  while the dimple depth was kept constant at 20  $\mu\text{m}$ . The results of these experiments are presented in Figure 2. The data shows that static friction continuously increases with decreasing dimple diameter by about a factor of 4 (from 0.91 N for a diameter of 200  $\mu\text{m}$  to 3.52 N for 20  $\mu\text{m}$ ). For the smallest diameter, static friction is even higher than that of the polished, untextured control.

That static friction increases with decreasing dimple diameter was somewhat unexpected but extremely fascinating and of

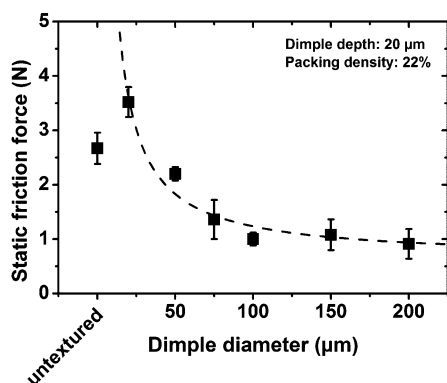


**Figure 2.** Static friction as a function of dimple diameter. Static friction was measured for untextured and laser surface textured brass samples against sapphire substrates at a normal load of 10 N. The depth (20  $\mu\text{m}$ ) and the packing density (22%) of the dimples were kept constant. The dimple diameter was varied between 20 and 200  $\mu\text{m}$ . The dashed line indicates a fit of the form  $f(x) = a + b/x$ , derived from fracture mechanics considerations. The error bars are the standard deviation from at least 120 measurements for each data point.

high relevance as it indicates that there is indeed contact splitting for dimpled surfaces under a tribological load. A very similar trend had been reported for the adhesion of elastomeric samples<sup>9</sup> patterned with dimples and pillars. There, the authors found that the pull-off force scaled linearly with the real contact perimeter of both texturing features. This picture, which did successfully explain the contact splitting for pull-off forces, cannot be directly applied to our situation of sliding surfaces and was also revisited by the authors, who later explained his behavior through a scaling with the contact area.<sup>10</sup> One also has to keep in mind that these studies were performed with elastomeric samples having an up to 5 orders of magnitude lower Young's modulus than our samples so that these results do not directly relate to ours. Our approach is based on viewing the transition from static to dynamic friction as a mode II crack moving through the interface between the sapphire disc and the brass sample. The dynamics of this cracklike front moving through the interface of the two sliding partners at the transition from static to dynamic friction have been studied by Fineberg and co-workers,<sup>20–22</sup> and also been modeled successfully.<sup>23</sup> Even though the experimental studies have been conducted on PMMA samples of significantly higher roughness than our contact materials, we think it is safe to expect a very similar crack front behavior in our experiments. This crack front moves through the interface on an extremely well-defined path that it cannot leave and there interacts with the dimples. At the very beginning of an experiment, the dimples will help to initiate the shear crack because of the stress concentrations at the dimples. The question thus is whether the dimples can also pin the crack, in analogy to particles pinning a dislocation. To answer this question, we consider the situation that the shear crack approaches a dimple. First, the dimple will increase the crack length which results in an increased driving force for crack motion and ultimately in lower static friction values compared to polished samples. The next step that has to be considered is that the crack also has to leave the dimple. Here, at the trailing edge of the dimple, in addition to the stress concentration in shear (mode II direction), the normal load of the contact and the geometry of the dimple result in a stress concentration in negative mode I direction. The magnitude of this stress concentration can be calculated following an

argument brought forward by Inglis for the stress concentrations around an elliptical hole in 1913.<sup>24</sup> He found that for the stress concentration in negative mode I direction  $\sigma_{yy}$ , we can write

$$\sigma_{yy} = \sigma_1(1 + 2(c/b)) \quad (1)$$

where  $\sigma_1$  is the applied tension and  $b$  and  $c$  are the semimajor axes of elliptical hole. In this picture,  $c$  corresponds to the dimple radius and as the dimple depth in our experiments was kept constant, so is  $b$ . Following this argument, we have a mixed-mode crack moving through the interface and the larger the dimple diameter, the higher the stress concentration in negative mode I direction at the dimple edge which will pin the crack from further movement. A longer crack front in the interface will be associated with a higher system energy and we can—in analogy with the Orowan model for dislocations<sup>25</sup>—attribute a “line tension” to the crack. For dislocations, the Orowan model states that the increase in shear tension  $\Delta\tau_{or}$  necessary to move the dislocation through the crystal is proportional to  $1/L$ , with  $L$  being the distance between the obstacles pinning the dislocation. In our experiments, the lateral spacing between the dimples is equal to their diameter. This straightforward fracture mechanics based model thus directly explains the  $1/\text{diameter}$  scaling presented in Figure 2. A similar approach was taken in the literature when thinking about the pull-off behavior of morphologically textured, fibrillar structures where a mode I crack moves through an interface and interacts with individual surface features, e.g., pillars.<sup>1</sup> Ben-David and Fineberg argue that fracture initiation and thus the transition from static to dynamic friction is determined by an energy balance similar to the one made when deriving the Griffith criterion for fracture.<sup>26</sup> They propose that the threshold for fracture strongly decreases when the length of the initially imposed “seed” crack is increased.<sup>26</sup> One could argue that our dimples act as such “seed” cracks and that thus the larger the dimples, the lower the static friction force. This is in agreement with the data presented in Figure 2.

As a second geometric parameter possibly influencing static friction values, we varied the dimple depth between 10 and 65  $\mu\text{m}$  while keeping the dimple diameter constant at 50  $\mu\text{m}$ . In Figure 3, the results of these experiments are presented (static friction as a function of dimple depths). For dimple depths

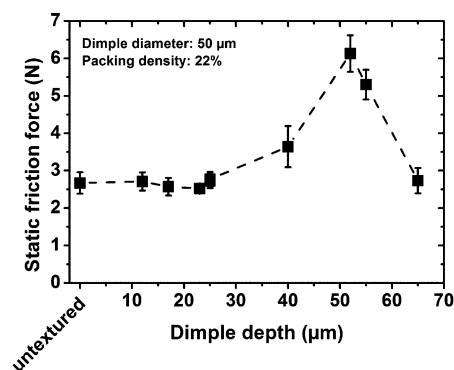


**Figure 3.** Static friction as a function of dimple depth. Static friction was measured for untextured and laser surface textured brass samples against sapphire substrates. The diameter (50  $\mu\text{m}$ ) and the packing density (22%) of the dimples were kept constant. The dimple depth was varied between 10 and 65  $\mu\text{m}$ . The dashed line was added to guide the eye.



from 10  $\mu\text{m}$  up to 25  $\mu\text{m}$ , static friction force is about the same as for the polished, untextured control sample. Then, friction values increase by more than a factor of 2 (from 2.67 N for the untextured case to 6.13 N for dimples being 52  $\mu\text{m}$  deep). When increasing the dimple depth further, static friction decreases again, roughly down to the value of the untextured sample (2.73 N for 65  $\mu\text{m}$  deep dimples).

Staying within the picture of a mixed mode crack moving through the interface, one could argue that the deeper the dimples, the smaller the effective shear stiffness of the material between them. Consequently, the struts tilt under the applied shear load, increasing the mode I stress concentrations resulting in a higher static friction force. The opposite trend is expected from the increase in  $b$  in eq 1 with increasing dimple depth. This should lead to a decrease in  $\sigma_{yy}$  and consequently a decrease in static friction with increasing dimple depth.

In the in situ experiments by Rubinstein et al., the crack was always initiated at the trailing edge of the sample,<sup>20</sup> but this has not to be the case in all of our experiments. It is possible that due to a different compliance of the dimple edge with increasing depth, a transition from a tension- to a compression-controlled crack initiation is observed, explaining the maximum seen in Figure 3. Also the energy balance criterion proposed by Ben-David and Fineberg will have to be considered.<sup>26</sup> So far we have no direct way to discriminate between the explanations. We will have to establish a high-speed in situ setup to do so.

When morphologically textured surfaces are at play, one could argue that changes in contact angle and capillary effects might be a possible explanation for the results presented here, similar to effects reported for fibrillar adhesives,<sup>27</sup> or single-asperity frictional contacts.<sup>28</sup> However, one has to keep in mind that in our case to contact area remains connected and that thus, one would not expect there to be individual capillary bridges, so that no scaling is expected with capillary forces. Nonetheless, capillary condensation will occur with our experimental conditions. This is why we kept the relative humidity constant for all experiments. For the future, it would be very interesting to repeat our experiments in vacuum conditions or dry nitrogen atmosphere in order to rule out capillary constitutions entirely. In order to investigate the influence of our textures on the wetting behavior, we performed contact angle measurements with static water droplets. The results of these experiments are presented in Figures S3 in the Supporting Information section. They show that neither dimple diameter nor depth significantly changes the contact angle, but that the mere texturing itself decreases the wettability of the brass surfaces from a static contact angle of 55 to 90°.

In conclusion, the morphological texturing of brass surfaces with dimples from 20 to 200  $\mu\text{m}$  in diameter, and depths from 10 to 65  $\mu\text{m}$  had a strong effect on the transition from static to dynamic friction. When reducing the diameter from 200 to 20  $\mu\text{m}$ , a contact splitting phenomenon occurred and an increase in static friction from 0.91 to 3.52 N (a factor of 4) was measured. This size and contact splitting effect was explained through introducing a line tension of the crack which moves through the interface between sapphire and brass in a mode II fashion. Because of stress concentrations at the dimple edges, an additional stress in negative mode I direction is applied, pinning the crack to the dimple. The additional shear stress necessary to overcome this pinning effect, scales inversely with the dimple diameter. When increasing the dimple depth,

friction reached a local maximum for a depth of 52  $\mu\text{m}$  and at a factor of 2 higher forces than for the polished controls.

These results are not only interesting from a mere contact mechanics point of view, where the sliding behavior of dimpled surfaces is a fascinating new field and a contact splitting phenomenon has not been reported before, but also have extremely high relevance in tribological contacts of different length scales. From micro- and nanoelectromechanical systems<sup>29,30</sup> to engines in automobiles,<sup>15</sup> laser surface texturing has received a lot of attention in past years because of its high potential to reduce friction and wear. Whether or not these contacts are lubricated, at the dead centers of a reciprocating contact or when a tribological system stops and starts again, true solid–solid contacts occur. Our data demonstrate that at certain combinations of dimple diameter and depth a strong increase in static friction may occur, which will increase friction dramatically and limit the lifetime of the components because of higher wear. Therefore, static friction data has to be taken into account when searching for the optimum dimple dimensions. On the other hand, there might be applications where high friction forces are favorable and the size effect investigated here can be exploited. Future research will investigate the effect of different normal loads and packing densities in order to further test the hypotheses proposed here.

## ■ ASSOCIATED CONTENT

### Supporting Information

A single static friction test, a white light interferometry profile of an entire sample after laser surface texturing, and static contact angles as a function of dimple diameter and depth, as well as the exact laser process parameters. This material is available free of charge via the Internet at <http://pubs.acs.org>.

## ■ AUTHOR INFORMATION

### Corresponding Author

\*E-mail: greiner@kit.edu.

### Notes

The authors declare no competing financial interest.

## ■ ACKNOWLEDGMENTS

This work was funded by the German Research Foundation DFG under Project GR 4174/1-1. We thank S. Blassmann and P. Schreiber for help with the laser surface texturing. Discussions with D. Braun and Dr. Johannes Schneider are greatly acknowledged.

## ■ REFERENCES

- (1) Boesel, L. F.; Greiner, C.; Arzt, E.; del Campo, A. Gecko-Inspired Surfaces: A Path to Strong and Reversible Dry Adhesives. *Adv. Mater.* **2010**, *22*, 2125–2137.
- (2) Autumn, K.; Liang, Y. A.; Hsieh, S. T.; Zesch, W.; Chan, W. P.; Kenny, T. W.; Fearing, R.; Full, R. J. Adhesive Force of a Single Gecko Foot-Hair. *Nature* **2000**, *405*, 681–685.
- (3) Autumn, K.; Sitti, M.; Liang, Y. C. A.; Peattie, A. M.; Hansen, W. R.; Sponberg, S.; Kenny, T. W.; Fearing, R.; Israelachvili, J. N.; Full, R. J. Evidence for van der Waals Adhesion in Gecko Setae. *Proc. Natl. Acad. Sci. U. S. A.* **2002**, *99*, 12252–12256.
- (4) Spolenak, R.; Gorb, S.; Gao, H. J.; Arzt, E. Effects of Contact Shape on the Scaling of Biological Attachments. *Proc. R. Soc. London, Ser. A* **2005**, *461*, 305–319.
- (5) Huber, G.; Mantz, H.; Spolenak, R.; Mecke, K.; Jacobs, K.; Gorb, S. N.; Arzt, E. Evidence for Capillarity Contributions to Gecko Adhesion from Single Spatula Nanomechanical Measurements. *Proc. Natl. Acad. Sci. U.S.A.* **2005**, *102*, 16293–16296.

- (6) Arzt, E.; Gorb, S.; Spolenak, R. From Micro to Nano Contacts in Biological Attachment Devices. *Proc. Natl. Acad. Sci. U. S. A.* **2003**, *100*, 10603–10606.
- (7) Greiner, C.; Del Campo, A.; Arzt, E. Adhesion of Bioinspired Micropatterned Surfaces: Effects of Pillar Radius, Aspect Ratio and Preload. *Langmuir* **2007**, *23*, 3495–3502.
- (8) Sameoto, D.; Menon, C. Recent Advances in the Fabrication and Adhesion Testing of Biomimetic Dry Adhesives. *Smart Mater. Struct.* **2010**, *19*, 103001.
- (9) Varenberg, M.; Peressadko, A.; Gorb, S.; Arzt, E. Effect of Real Contact Geometry on Adhesion. *Appl. Phys. Lett.* **2006**, *89*, 121905.
- (10) Varenberg, M.; Murarash, B.; Kligerman, Y.; Gorb, S. N. Geometry-Controlled Adhesion: Revisiting the Contact Splitting Hypothesis. *Appl. Phys. A: Mater. Sci. Process.* **2011**, *103*, 933–938.
- (11) Etsion, I. *State of the Art in Laser Surface Texturing*; Tsinghua University Press: Beijing, 2009.
- (12) Borghi, A.; Gualtieri, E.; Marchetto, D.; Moretti, L.; Valeri, S. Tribological Effects of Surface Texturing on Nitriding Steel for High-Performance Engine Applications. *Wear* **2008**, *265*, 1046–1051.
- (13) Andersson, P.; Koskinen, J.; Varjus, S.; Gerbig, Y.; Haefke, H.; Georgiou, S.; Zhmud, B.; Buss, W. Microlubrication Effect by Laser-Textured Steel Surfaces. *Wear* **2007**, *262*, 369–379.
- (14) Etsion, I. State of the Art in Laser Surface Texturing. *J. Tribol.—Trans. ASME* **2005**, *127*, 248–253.
- (15) Etsion, I.; Sher, E. Improving Fuel Efficiency with Laser Surface Textured Piston Rings. *Tribol. Int.* **2009**, *42*, 542–547.
- (16) Etsion, I.; Burstein, L. A Model for Mechanical Seals with Regular Microsurface Structure. *Tribol. Trans.* **1996**, *39*, 677–683.
- (17) Zum Gahr, K. H.; Wahl, R.; Wauthier, K. Experimental Study of the Effect of Microtexturing on Oil Lubricated Ceramic/Steel Friction Pairs. *Wear* **2009**, *267*, 1241–1251.
- (18) Mourier, L.; Mazuyer, D.; Lubrecht, A. A.; Donnet, C. Transient Increase of Film Thickness in Micro-Textured EHL Contacts. *Tribol. Int.* **2006**, *39*, 1745–1756.
- (19) Poser, K.; Zum Gahr, K. H.; Schneider, J. Development of Al<sub>2</sub>O<sub>3</sub> Based Ceramics for Dry Friction Systems. *Wear* **2005**, *259*, 529–538.
- (20) Rubinstein, S. M.; Cohen, G.; Fineberg, J. Detachment Fronts and the Onset of Dynamic Friction. *Nature* **2004**, *430*, 1005–1009.
- (21) Rubinstein, S. M.; Cohen, G.; Fineberg, J. Contact Area Measurements Reveal Loading-History Dependence of Static Friction. *Phys. Rev. Lett.* **2006**, *96*, 256103.
- (22) Ben-David, O.; Rubinstein, S. M.; Fineberg, J. Slip-Stick and the Evolution of Frictional Strength. *Nature* **2010**, *463*, 76–79.
- (23) Bouchbinder, E.; Brener, E. A.; Barel, I.; Urbakh, M. Slow Cracklike Dynamics at the Onset of Frictional Sliding. *Phys. Rev. Lett.* **2011**, *107*, 235501.
- (24) Inglis, C. E. Stresses in a Plate Due to the Presence of Cracks and Sharp Corners. *Trans. Inst. Nav. Archit.: Eng.* **1913**, *95*, 415.
- (25) Hull, D.; Bacon, D. J. *Introduction to Dislocations*, fifth ed.; Butterworth-Heinemann: Oxford, U.K., 2011.
- (26) Ben-David, O.; Fineberg, J. Static Friction Coefficient Is Not a Material Constant. *Phys. Rev. Lett.* **2011**, *106*, 254301.
- (27) Buhl, S.; Greiner, C.; Del Campo, A.; Arzt, E. Humidity Effect on Adhesion of Microstructured Elastomer Surfaces. *Int. J. Mater. Res.* **2009**, *100*, 1119–1126.
- (28) Greiner, C.; Felts, J. R.; Dai, Z.; King, W. P.; Carpick, R. W. Local Nanoscale Heating Modulates Single-Asperity Friction. *Nano Lett.* **2010**, *10*, 4640–4645.
- (29) Xuan, J.; Shih, C.; Pan, Z.; Nguyen, T.; Yang, S. Optimization of Bump Shape and Pattern in Laser-Texture Design for Improving Media Tribological Performance. *IEEE Trans. Magn.* **1999**, *35*, 2436–2438.
- (30) Tay, N. B.; Minn, M.; Sinha, S. K. A Tribological Study of SU-8 Micro-Dot Patterns Printed on Si Surface in a Flat-on-Flat Reciprocating Sliding Test. *Tribol. Lett.* **2011**, *44*, 167–176.